Annals of R.S.C.B., ISSN:1583-6258, Vol. 25, Issue 6, 2021, Pages. 6894 - 6902
Received 25 April 2021; Accepted 08 May 2021.

Role of Bioconvection on Nanofluid Flow in a Thin Moving Needle in the Effect of Soret and Dufour

I Sadham Hussain[1], D Prakash[2,*]
[1,2]Department of Mathematics, College of Engineering and Technology, Faculty of Engineering and Technology, SRM Institute of Science and Technology, SRM Nagar, Kattankulathur -603203, TN, India.
[1]sadhamhi@srmist.edu.in, [2,*]prakashd1@srmist.edu.in

ABSTRACT

The purpose of this article is to study the bioconvection in the flow of nanofluids due to the thin moving needle using the mathematical nanofluid model with soret and dufour effect. A similarity transformation is used to reduce the governing partial differential equations to a set of ordinary differential equations which are then solved numerically Runge–Kutta–Fehlberg method with shooting technique (RKSM) for various values of the governing parameters. The numerical values gained within the boundary layer for the dimensionless velocity, temperature, concentration, motile diffusivity number, heat transfer rate and mass transfer rate are presented through graphs and tables for some set of values of governing parameters.

Keywords: Nanofluid, Soret, Dufour, Thin moving needle, Brownian motion.

Introduction

Soret and Dufour effects are analyzed to have a look at the thermo-diffusion and diffusion-thermo influences at the drift. The Soret impact is the contribution to the mass fluxes because of temperature gradients. In blended heat and mass transfer techniques, the thermal energy flux attributable to concentration gradients is referred to as the Dufour or diffusion–thermal effect. Both Soret and Dufour impacts become huge when species are presented on a superficial level in a fluid area with a lower thickness than the encompassing fluid. There are numerous works which have been published to expose the importance of Soret and Dufour effects at the nanofluid flow, for example [1-5]. Furthermore, the uses of Soret and Dufour effects can be found in the space of reactor safety, ignition flares and sun based authorities just as building energy protection.

The wonder of bioconvection has emerged because of the variety of density gradient related to the development of plainly visible convective fluid particles. As a feature of this interaction, the density of the base liquid is shortened. Platt [6] first coined the term “bioconvection” which describes the flow patterns observed in the culture of free-swimming species in 1961. Recently, particular attention has been given to this phenomenon, as it implies many practical applications in biotechnology, bio-microsystems and bio-sciences. Besides, it has as of late been seen that the utilization of bioconvection with nanoparticles is more compelling at improving the stability of nanoparticles. These micro-organisms self-propelled in a particular direction improve the density of the fluids and thus induce bioconvection. This new theory was started by Kusznetsov [7-9].

In the course of the most recent couple of years, attributable to the notable application in industry, nanofluids have interested the consideration of specialists. The ordinary warmth move in fluids can't offer the suitable cooling measures in industries. These instances lead to an expansion of nanotechnology. Collision of nanoparticles has several element and essential characteristics in the producing of paints, ceramics, drugs delivery systems, food coatings and etc. Some recognized examination considers referencing the novel attributes of thin needle because of various sorts of stream can be found in references [10-15]. Heat transfer at multiple surface temperatures using a thin needle was studied predominately by Grosan and Pop [16]. Furthermore, the flow of a nanofluid by contemplating prescribed surface heat flux has been achieved by Waini et al. [17].

In this paper, the novelty of the present work is to investigate the slender needle moving of bioconvective nanofluid with soret and dufour effect. The governing partial differential equations are converted into ordinary differential equations by using the similarity transformations, and then are solved numerically by RKSM. A careful review of existing work reveals that no one has attempted the Soret and Dufour effect on bioconvective steady flow of Buongiorno’s nanofluid over a thin moving needle. Present numerical results has been comparing with existing result.

Annals of R.S.C.B., ISSN:1583-6258, Vol. 25, Issue 6, 2021, Pages. 6894 - 6902
Received 25 April 2021; Accepted 08 May 2021.

Mathematical formulation

We assume the steady state laminar, boundary layer flow, heat and mass transfer characteristics of nanofluid over a thin moving needle with constant velocity u_w and free stream velocity u_∞. The composite velocity u is assumed to be the combinations of needle velocity u_w and free stream velocity u_∞. Flow velocities *u* and *v* are taken in the direction of axes x and r axes respectively, as shown in fig.1. A thin needle has been chosen so that it not exceeds momentum and thermal boundary layer. With the assumption of negligible pressure gradient along the needle, the function $r = R(x) = \sqrt{\frac{vcx}{U}}$ specifies the shape of the thin needle where the surface of needle is maintained at uniform temperature $T_w (> T_\infty)$ and concentration $C_w (> C_\infty)$, we have following governing equation is :

$$\frac{\partial}{\partial x}(ru) + \frac{\partial}{\partial r}(r\mathrm{v}) = 0 \tag{1}$$

$$u\frac{\partial u}{\partial x} + \mathrm{v}\frac{\partial u}{\partial r} = \frac{\nu}{r}\frac{\partial}{\partial x}\left(r\frac{\partial u}{\partial x}\right) \tag{2}$$

$$u\frac{\partial T}{\partial x} + \mathrm{v}\frac{\partial T}{\partial r} = \frac{\alpha}{r}\frac{\partial}{\partial r}\left(r\frac{\partial T}{\partial r}\right) + \tau\left(D_B\frac{\partial T}{\partial x}\frac{\partial C}{\partial x} + \frac{D_T}{T_\infty}\left(\frac{\partial T}{\partial r}\right)^2\right) + \frac{D_m}{C_p C_s}\frac{1}{r}\frac{\partial}{\partial x}\left(r\frac{\partial C}{\partial x}\right) \tag{3}$$

$$u\frac{\partial C}{\partial x} + \mathrm{v}\frac{\partial C}{\partial r} = \frac{D_B}{r}\frac{\partial}{\partial r}\left(r\frac{\partial C}{\partial r}\right) + \frac{D_T}{T_\infty}\frac{1}{r}\frac{\partial}{\partial r}\left(r\frac{\partial T}{\partial r}\right) + \frac{D_m k_T}{T_m}\frac{1}{r}\frac{\partial}{\partial x}\left(r\frac{\partial T}{\partial x}\right) \tag{4}$$

$$u\frac{\partial N}{\partial x} + \mathrm{v}\frac{\partial N}{\partial r} + \frac{bWc}{r}\frac{\partial}{\partial r}\left(r\frac{\partial C}{\partial r}\right) = Dn\frac{\partial^2 N}{\partial r^2} \tag{5}$$

The boundary condition associated with equations (1-5)

$$u = u_w, \mathrm{v} = 0, T = T_w, C = C_w, \; N = N_w \; at \; r = R(x)$$
$$u \to u_\infty, T \to T_\infty, C \to C_\infty, \; N \to N_\infty \; as \; r \to \infty \tag{6}$$

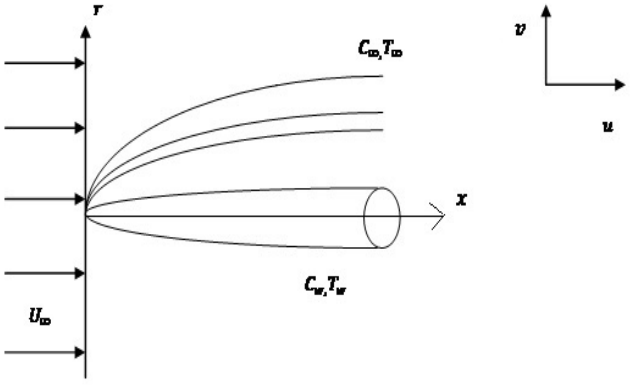

Figure 1. Physical model of the present study

Where, Sr is the Soret number, Du is the Dufour number, ν is the kinematic viscosity, α is the thermal diffusivity, τ is the ratio of nanofluid effective heat capacity, C and T and are the concentration and temperature of nanofluid respectively, D_T stands for thermophoretic diffusion coefficient, D_B stands for Brownian diffusion coefficient
Considering the appropriate similarity variable,

$$\eta = \frac{Ur^2}{\nu x}, \psi = \nu x f', \phi(\eta) = \frac{C - C_\infty}{C_\infty}, \theta(\eta) = \frac{T - T_\infty}{T_w - T_\infty} \tag{7}$$

Where $u = \frac{1}{r}\frac{\partial \psi}{\partial r}$ and $\mathrm{v} = -\frac{1}{r}\frac{\partial \psi}{\partial x}$. Eqs. (2) – (4) transform into the ordinary differential equations.

$$ff' + 2\eta f''' + 2f'' = 0 \tag{8}$$

$$\frac{2}{Pr}(\eta\theta'' + \theta') + 2\eta\left(Nt\,\theta'^2 + Nb\theta'\phi'\right) + f\theta' + Du(2\eta\phi' + 2\eta\phi'') = 0 \tag{9}$$

$$Scf\phi' + 2(\phi' + \eta\phi'') + 2\frac{Nt}{Nb}(\eta\theta'' + \theta') + 2LeSr(\eta\theta'' + \theta') = 0 \tag{10}$$

Annals of R.S.C.B., ISSN:1583-6258, Vol. 25, Issue 6, 2021, Pages. 6894 - 6902
Received 25 April 2021; Accepted 08 May 2021.

$$2\eta\chi^{"} + \chi^{'} + Lbf\chi^{'} - Pe(\phi^{'}(\chi + 2\eta\chi^{'} + \Omega) + \phi^{"}(2\eta\chi + 2\eta\Omega) = 0 \quad (11)$$

Here Sc represents the Schmidt number, *Nb* the Brownian motion parameter, Pr denotes the Prandtl number and *Nt* the thermophoresis parameter are signified as

$$Pr = \frac{\nu}{\alpha}, Sc = \frac{\nu}{D_B}, Nb = \frac{\tau D_B C_\infty}{\nu}, Nt = \frac{\tau D_T (T_w - T_\infty)}{\nu T_\infty}, E = \frac{E_a}{kT_\infty}, \delta = \frac{T_w - T_\infty}{T_\infty},$$
$$Lb = \frac{\nu}{D_n},\ Pe = \frac{bW_c}{D_n},\ \Omega = \frac{N_w}{N_w - N_\infty}\ , \quad (12)$$

The transformed boundary conditions are:

$$f = \frac{\lambda a}{2}\ , f^{'} = \frac{\lambda}{2}, \theta = 1, \phi = 1, \chi = 1\ at\ \eta = a$$
$$f^{'} = \frac{1-\lambda}{2}, \theta \to 0, \phi \to 0, \chi\ \to 0\ at\ \eta \to \infty \quad (13)$$

Which the λ parameter is the ratio of needle velocity to composite velocity, If $\lambda=0$, then the status of static needle in a moving nanofluid and $\lambda=1$ shows the case of moving needle in an inactive ambient fluid. The physical aspects of the pre-eminent interest of the momentum, thermal distribution, volume fraction of concentration in the presented paper are local Nusselt number, skin-friction, local Sherwood number, motile density number which are respectively denoted by $Nu,\ C_f$, *Sh*, *Nn*.

The dimensionless form of Nusselt number, Sherwood number, motile density number can be written as

$$Nu = -2Re^{\frac{1}{2}}a^{\frac{1}{2}}\theta^{'}(a), Sh = -2Re^{\frac{1}{2}}a^{\frac{1}{2}}\phi^{'}(a), \quad Nn = -2Re^{\frac{1}{2}}a^{\frac{1}{2}}\chi^{'}(a) \quad (14)$$

Numerical solution

In this present study, the governing Equations (8) - (11) with boundary conditions (13) are solved numerically using Runge–Kutta–Fehlberg method with shooting technique for different parameters. To solve the governing equations, the shooting technique is that which is easy to implement and the results in convincing accuracy. Before commencing the simulation, Boundary value problem is converted to Initial value problem as follows.

$$f = y_1, f^{'} = y_2, f^{''} = y_3, \theta = y_4, \theta^{'} = y_5, \phi = y_6, \phi^{'} = y_7, \chi = y_8, \chi^{'} = y_9 \quad (15)$$

$$y_1^{'} = y_2;$$
$$y_2^{'} = y_3;$$
$$y_3^{'} = \frac{1}{2\eta}(-2y_3 - y_1y_3);$$
$$y_4^{'} = y_5;$$
$$y_5^{'} = \frac{Pr}{2\eta}\left(-\frac{2y_5}{Pr} - 2\eta\left(Nty_5^{'} + Nby_5y_7\right) - y_1y_5 + Du(2\eta y_7^{'} + 2\eta y_7\right); \quad (16)$$
$$y_6^{'} = y_7;$$
$$y_7^{'} = -\frac{1}{2\eta}\left(2y_7 + 2\frac{Nt}{Nb}(\eta y_5^{'} + y_5) + Scy_1y_7 + 2LeSr(y_5 + \eta y_5^{'})\right);$$
$$y_8^{'} = y_9;$$
$$y_9^{'} = -\frac{1}{2\eta}\left(-y_9 - Lby_1y_9 + Pe(y_7(y_8 + 2\eta y_9 + \Omega) + y_7^{'}(2\eta y_8 + 2\eta\Omega)\right);$$

The transformed conditions are

$$y_1(\eta) = \frac{\lambda a}{2}, y_2(\eta) = \frac{\lambda}{2}, y_3(\eta) = g_1, y_4(\eta) = 1, y_5(\eta) = g_2\ \ y_6(\eta) = 1,$$
$$y_7(\eta) = g_3, y_8(\eta) = 1, y_9(\eta) = g_4\ ;\ as\ \eta = a \quad (17)$$

$$y_2(\eta) = \frac{1-\lambda}{2}, y_4(\eta) = 0, y_6(\eta) = 0,\ y_8(\eta) = 0\ as\ \eta \to \infty; \quad (18)$$

Annals of R.S.C.B., ISSN:1583-6258, Vol. 25, Issue 6, 2021, Pages. 6894 - 6902
Received 25 April 2021; Accepted 08 May 2021.

Results and Discussion

Overall the results to be declared below, the default values of the parameters are considered as λ =0.1, a=0.1, Nt=0.1, Nb=0.1, Ω=0.2, Lb=0.1, Sr=0.1, Du=0.2, Sc=0.5, Pr=7, Pe=0.1, Le=0.5 unless otherwise specified. The impact of λ on profiles of f' is presented in Figure. 2. f' increases monotonically with similarity variable η when $0 \le \lambda < 0.5$ while a monotonically decrease in f' with an increase in η is observed for $\lambda > 0.5$. Furthermore the velocity rises just near the needle surface and decreases far from it when λ is increased. It is very obvious from Figure. 3 that augmentation in the velocity parameter λ is responsible for the decrease in the temperature profile of the nanofluid.

Table 1 Comparison values of f'' for different values of *a*

a	Sallah et al [5]	Ahamed et al [15]	Present
0.01	8.4924452	8.4924360	8.4919404
0.1	1.2888300	1.2888171	1.2888277

Table 2 Numerical values for Nusselt number and Sherwood number for different values of *Sr* and *Du*

Sr	*Du*	Sallah et al [5]		Present	
		Nu	Sh	Nu	Sh
0.15	0.4	1.128098	1.744037	1.127541	1.743232
0.3	0.2	1.173818	1.758622	1.174713	1.757636
0.6	0.1	1.193840	1.832522	1.194327	1.831611

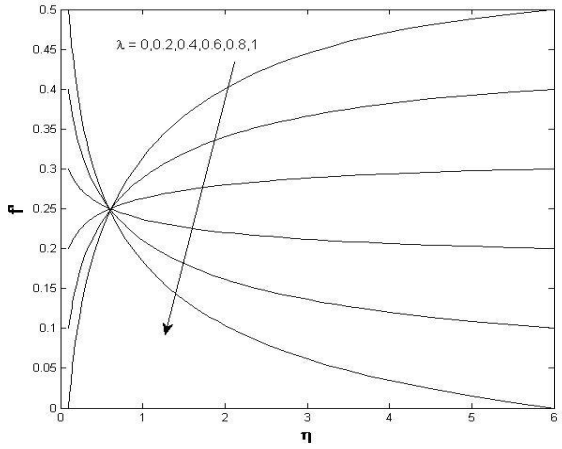

Figure 2. Velocity profile for different values of λ

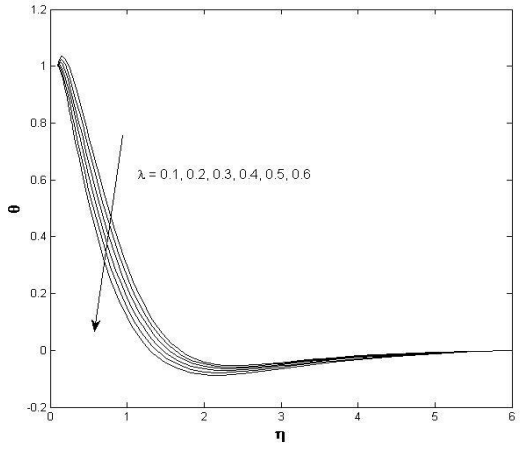

Figure 3. Temperature profile for different values of λ

Figure. 4 is drawn for temperature profile versus for different values of the Dufour number *Du*. We observed from this figure that the increase effect of Dufour number *Du* is to decrease the temperature distribution. In Figure. 5, it is viewed that an increment in Dufour number *Du*, significantly depreciates the concentration distribution ϕ. From Figure. 6 we examine the decreasing behavior of Soret number *Sr* against nanoparticles concentration profile. Figure.

Annals of R.S.C.B., ISSN:1583-6258, Vol. 25, Issue 6, 2021, Pages. 6894 - 6902
Received 25 April 2021; Accepted 08 May 2021.

7 shows that increase the Prandtl number increase with the enlargement in λ.

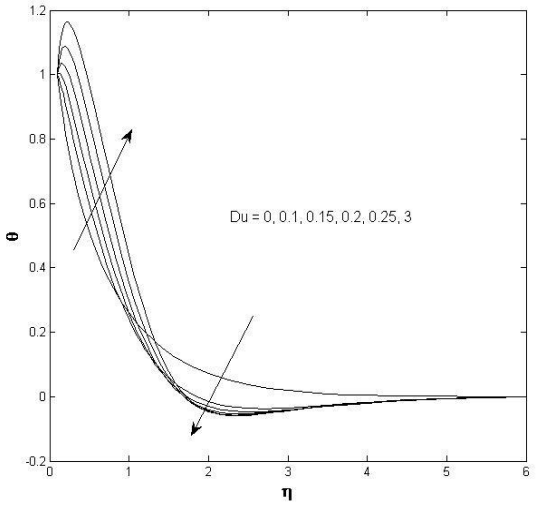

Figure 4. Temperature profile for different values of *Du*

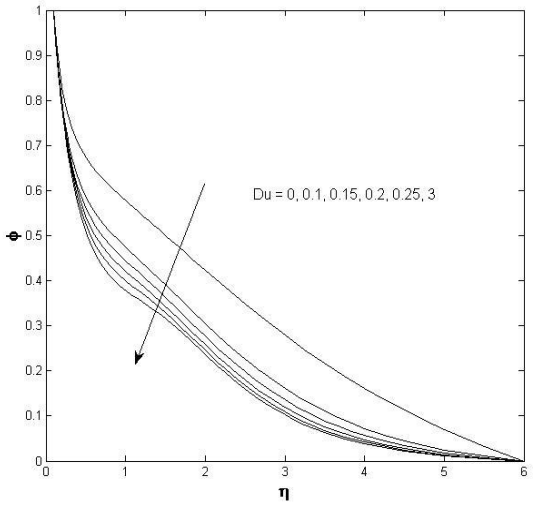

Figure 5. Concentration profile for different values of *Du*

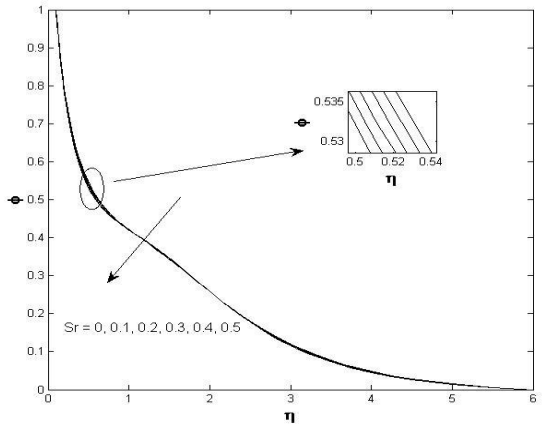

Figure 6. Concentration profile for different values of *Sr*

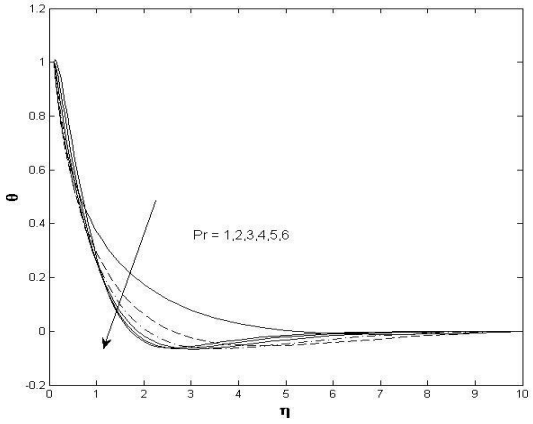

Figure 7. Temperature profile for different values of *Pr*

If two different non reacting fluids of the same temperature were released to diffuse in the system, then the difference in the temperature of the system increases. Figure. 10 are sketched to witness the impact of the Peclet number *Pe* on concentration profile ϕ. The motile organism concentration is decreased for large estimates *Pe*. It means that enhance concentration profile due to increase diffusive transport rate. In Fig. 11, it is noted that larger *Lb* increases the microorganism profile. Table 1 shows the comparison of the present with published work. It is revealed that the results of the present study are in a close agreement with the findings of Sallah et al. [5] and Ahamed et al. [15]. Table 2 depicts the numerically calculated values of Nusselt number and Sherwood number for numerous estimates of *Sr* and *Du* done by Sallah et al. [5]. An outstanding harmony between the results is found. That also validates the current exploration results. It is understood from the analysis of the numerical data enlisted in the Table 3 that Nusselt number, Sherwood number and motile density number for different parameter values.

Annals of R.S.C.B., ISSN:1583-6258, Vol. 25, Issue 6, 2021, Pages. 6894 - 6902
Received 25 April 2021; Accepted 08 May 2021.

Enhance the Sherwood number and motile density number as an increase in the *Sr* and *Du* number. Reverse trend happens in Nusselt number.

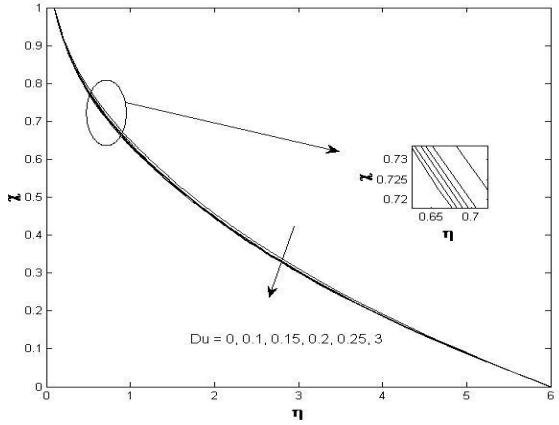

Figure 8. Concentration profile for different values of *Du*

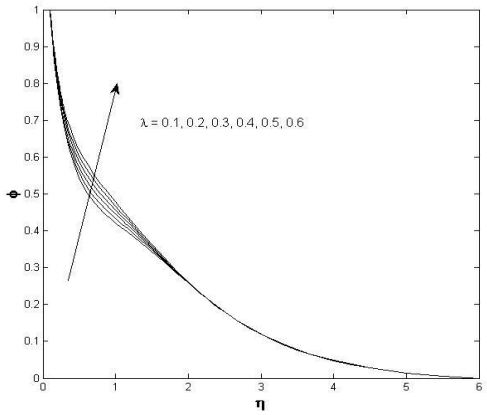

Figure 9. Concentration profile for different values of λ

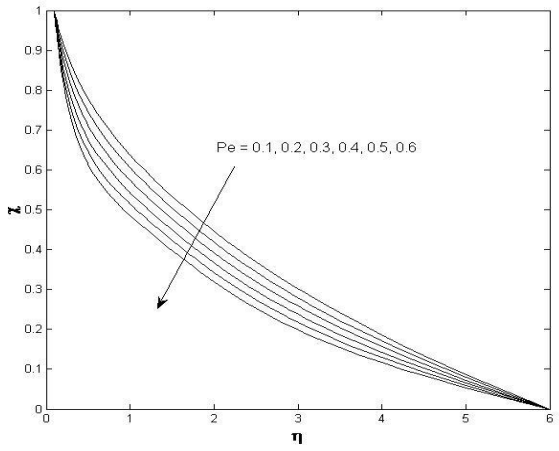

Figure 10. Concentration profile for different values of *Pe*

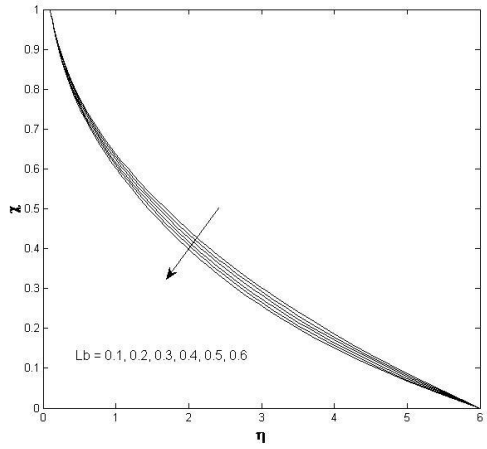

Figure 11. Temperature profile for different values of *Lb*

Table 3 Local Nusselt number, Sherwood number and motile density number for various values of parameter.

Sr	Du	Pe	Lb	Nb	Nt	λ	$(Re_x)^{-1/2}Nu$	$(Re_x)^{-1/2}Sh$	$(Re_x)^{-1/2}Nn$
0.1	0.2	0.1	0.1	0.1	0.1	0.1	-1.026664	1.893941	0.404101
0.2							-1.084603	1.917390	0.406890
0.3							-1.140852	1.939756	0.409551

Annals of R.S.C.B., ISSN:1583-6258, Vol. 25, Issue 6, 2021, Pages. 6894 - 6902
Received 25 April 2021; Accepted 08 May 2021.

	0.1						0.326340	1.881132	0.403101
	0.15						-0.327373	1.891786	0.404046
	0.25						-1.845790	1.921674	0.407281
		0.2					0.326340	1.881132	0.612208
		0.3					0.326340	1.881132	0.822526
		0.4					0.326340	1.881132	1.033974
			0.2				0.326340	1.881132	0.445829
			0.3				0.326340	1.881132	0.484832
			0.4				0.326340	1.881132	0.519865
				0.2			0.051875	1.835112	0.397573
				0.3			-0.163835	1.811377	0.394727
				0.4			-0.310155	1.787446	0.391858
					0.13		-0.020835	2.071187	0.425731
					0.15		-0.239108	2.182699	0.438977
					0.18		-0.541493	2.320725	0.455318
						0.2	0.476191	1.826297	0.393338
						0.3	0.635701	1.766323	0.382968
						0.4	0.804665	1.701309	0.372021

Conclusion

Here we have examined Soret and Dufour effect of bioconvection the nanofluid flow over a thin moving needle and Buongiorno nanofluid model utilized to express the flow equations. Temperature θ shows that it increases as velocity of the needle increases and higher Prandtl number fluid retains lower thermal diffusivity. Motile microorganism profile decreases due to increases in Dufour number. The concentration of the fluid increases with the increasing values of parameters *Sr*.

Reference

1) Salleh, S.N.A., Bachok, N., Arifin, N.M., Ali, F.M. (2019). A stability analysis of solutions on boundary layer flow past a moving thin needle in a nanofluid with slip effect, *ASM Science Journal* 12, pp. 60–70.
2) Pal, D., Mandal, G., & Vajravalu, K. (2016). Soret and dufour effects on MHD convective-radiative heat and mass transfer of nanofluids over a vertical non-linear

Annals of R.S.C.B., ISSN:1583-6258, Vol. 25, Issue 6, 2021, Pages. 6894 - 6902
Received 25 April 2021; Accepted 08 May 2021.

stretching/shrinking sheet, *Applied Mathematics and Computation*, 287/288, pp. 184-200.

3) Umavathi, J.C., Sheremet, M.A., Ojjela, O., & Reddy, G.J. (2017). The onset of double-diffusive convection in a nanofluid saturated porous layer: cross-diffusion effects, *European Journal of Mechanics - B/Fluids.* 65, pp. 70-87.
4) Haroun, N.A., Sibanda, P., Mondal, S., & Motsa, S.S. (2015). On unsteady MHD mixed convection in a nanofluid due to a stretching/shrinking surface with suction/injection using the spectral relaxation method, *Boundary Value Problems*. 1, pp. 1-17.
5) Salleh, S.N.A. (2020). Influence of Soret and Dufour on forced convection flow towards a moving thin needle considering Buongiorno's nanofluid model, *Alexandria engineering journal.* 59, pp. 3897-3906.
6) Platt, R. (1961). Bioconvection patterns in cultures of free-swimming organisms, *Science* 133, pp. 1766-1767.
7) Kuznetsov, A.V. (2010). The onset of nanofluid bioconvection in a suspension containing both nanoparticles and gyrotacticmicroorganisms, *International Communications in Heat and Mass Transfer* 106, 1421-1425.
8) Kuznetsov, A.V. (2011). Nanofluid bioconvection in water-based suspensions containing Nanoparticles and oxytactic microorganisms, oscillatory instability, Nanoscale Res. Lett. 6, 100.
9) Kuznetsov, A.V. (2011). Non-oscillatory and oscillatory nanofluid bio-thermal convection in a horizontal layer of finite depth, European Journal of Mechanics-B/Fluids 30, 156 – 165.
10) Lee, L.L. (1967). Boundary layer over a thin needle, Physics of Fluids 10, pp. 820-822.
11) Cebeci, T., Na, T.Y. (1969). Laminar free convection heat transfer from a needle, *Phys fluids 12*, pp. 463-465.
12) Afridi, M.I., Qasim, M. (2018). Entropy generation and heat transfer in boundary layer flow over a thin needle moving in a parallel stream in the presence of nonlinear Rosseland radiation, *Int. J. Therm. Sci.*, 123, pp. 117-128.
13) Soid, S.K., Ishak, A., & Pop. I. (2017). Boundary layer flow past a continuously moving thin needle in a nanofluid, *Appl. Therm. Eng.*, 114, pp. 58-64.
14) Hayat, T., Khan, M.I., Farooq, M., Yasmeen, T., Alsaedi, A. (2016). Water-carbon nanofluid flow with variable heat flux by a thin needle. *J. Mol. Liq.*, 224, pp. 786–791.
15) Ahmad, R., Mustafa, M. (2017). Buongiorno's model for fluid flow around a moving thin needle in a flowing nanofluid: A numerical study. *Chin. J. Phys.*, 55, pp. 1264–1274.
16) Grosan, T., Pop, I. (2011). Forced Convection Boundary Layer Flow Past Non isothermal Thin Needles in nanofluids. *J. Heat Trans*, 133, pp. 054503-054507.
17) Waini, A., Ishak, A., & Pop, I. (2019). On the stability of the flow and heat transfer over a moving thin needle with prescribed surface heat flux. *Chin. J. Phys.*, 60, pp. 651–658.
18) Choi, S.U.S. (1995). Enhancing thermal conductivity of fluids with nanoparticles, D.A. Siginer, H.P. Wang (Eds.), *Developments and Applications of Non-Newtonian Flows*, ASME FED. 231, pp. 99–105.

Annals of R.S.C.B., ISSN:1583-6258, Vol. 25, Issue 6, 2021, Pages. 6894 - 6902
Received 25 April 2021; Accepted 08 May 2021.

19) Kang, H.U., Kim, S.H., & Oh, J.M. (2006). Estimation of thermal conductivity of nanofluid using experimental effective particle volume, *Exp. Heat Transf.* 19, pp. 181–191.
20) Buongiorno, J. (2006). Convective transport in nanofluids, *ASME J. Heat Transf.* 128, pp. 240–250.
21) Hayat, T., Riaz, R., Aziz, A., & Alsaedi, A. (2020). Influence of Arrhenius activation energy in MHD flow of third grade nanofluid over a nonlinear stretching surface with convective heat and mass conditions. *Physica A* 549, p. 124006.
22) Hayat, T., Aziz, A., Muhammad, T., & Alsaedi, A. (2019). Effects of binary chemical reaction and Arrhenius activation energy in Darcy-Forchheimer three-dimensional flow of nanofluid subject to rotating frame, *J. Thermal Anal. Calorimet*. 136, pp. 1769–1779.
23) Hayat, T., Kha, S.A., Kha, M.L., & Alsaedi. A. (2019). Theoretical investigation of Ree–Eyring nanofluid flow with entropy optimization and Arrhenius activation energy between two rotating disks. *Computer Methods and Programs in Biomedicine* 177, pp. 57–68.
24) Bestman, A.R. (1990). Natural convection boundary layer with suction and mass transfer in a porous medium, *Int. J. Energy Res.* 14, pp. 389–396.
25) Makinde, O.D., Olanrewaju, P.O., & Charles. W.M. (2011). Unsteady convection with chemical reaction and radiative heat transfer past a flat porous plate moving through a binary mixture, *Afr. Mat*. 22, pp. 65-78.
26) Shafique, Z., Mustafa, M., & Mushtaq, A. (2016). Boundary layer flow of Maxwell fluid in rotating frame with binary chemical reaction and activation energy. *Results in Physics* 6, pp. 627–633.
27) Ishak, A., Nazar, R., & Pop, I. (2007). Boundary layer flow over a continuously moving thin needle in a parallel free stream. *Chin Phys Lett*, 24, pp. 2895-2897.
28) Chen, J.L.S., & Smith. T. N. (1978). Forced convection heat transfer from nonisothermal thin needles. *J Heat Transf*, 100, pp. 358-362.
29) Souayeh, B., Reddy, M. G., Sreenivasulu, P., Poornima, T., Mohammad Rahimi-Gorji, Ibrahim. M. Alarifi. (2019). Comparative analysis on non-linear radiative heat transfer on MHD Casson nanofluid past a thin needle. *Journal of Molecular Liquids* 284, pp. 163–174.